Shape evolution of a single liquid-crystal droplet immersed in an isotropic matrix under transient and steady flow

Youjun Wu, Wei Yu,* and Chixing Zhou
Department of Polymer Science and Engineering, Advanced Rheology Institute, Shanghai Jiao Tong University, Shanghai 200240, People's Republic of China

Yuanze Xu
Department of Macromolecular Science, Fudan University, Shanghai 200433, People's Republic of China
(Received 11 December 2006; published 26 April 2007)

The morphology evolution of immiscible polymer-liquid crystal systems is quite different from flexible polymer-polymer mixtures due to the anisotropic properties of liquid crystals. The deformation and retraction of a single low molar mass liquid crystal 4′-pentyl-4-biphenylcarbonitrile (5CB) droplet and 4′-octyl-4-biphenylcarbonitrile (8CB) dispersed in polydimethyl-siloxane under two-dimensional linear flow was investigated by a computer-controlled four-roll mill, which is equipped with an optical microscope and a digital camera. The deformation parameter and orientation angle during deformation versus capillary number was obtained and compared with calculations using the Maffettone-Minale (MM) model and the Yu-Zhou liquid-crystal (YZ-LC) model. The MM model can describe the behavior of a Newtonian droplet in another Newtonian matrix whereas the YZ-LC model can describe the behavior of a LC droplet in a Newtonian matrix. The results showed that the deformation and rotation of a LC droplet is more difficult than viscoelastic droplets, possibly because of the resistance of the nematic elastic energy induced by the nematic mesogens deformation and orientation under flow field. Furthermore, the different behavior between flow-aligning 5CB and flow-tumbling 8CB droplets and the influence of droplet size of LC on deformation and retraction were discussed by experiment and calculation; the results reveal that the different size LC droplets show different evolution curves.

DOI: 10.1103/PhysRevE.75.041706 PACS number(s): 61.30.Eb

I. INTRODUCTION

Liquid crystal (LC) dispersed in an amorphous liquid matrix is of great interest in a variety of applications. For example, in the developments of the polymer-dispersed liquid crystals for applications in flat panel television technology and switchable windows in display technology, dispersed liquid crystalline polymers act as "flow modifiers" for conventional thermoplastics, resulting in substantial reduction in extrusion pressure at very low concentration ($<5\%$) [1]. One of the essential steps in these kinds of mixing processes is the deformation and retraction of dispersed droplets in an immiscible matrix. In order to better control the properties of such materials, it is crucial to understand the dynamics of morphology evolution in such systems.

The dynamics of an isolated Newtonian or viscoelastic drop immersed in an immiscible Newtonian liquid phase undergoing shear flow has been the subject of a number of studies, both theoretical and experimental [2–4]. Two dimensionless numbers were found to influence the shape of droplets in flow field: The viscosity ratio $p=\eta_d/\eta_m$, η_d and η_m are viscosity of droplet and matrix, and the capillary number $\mathrm{Ca}=\eta_m R\dot{\gamma}/\Gamma$, R is the radius of droplet, $\dot{\gamma}$ the strain rate, and Γ the interfacial tension. When the viscosity ratio is given, the only crucial factor is the capillary number, which can be regarded as a ratio between the viscous shear stress ($\eta_m\dot{\gamma}$) and the interfacial tension (Γ/R). When one or both fluids become viscoelastic, the Deborah number $\mathrm{De}=\tau\dot{\gamma}$ starts to affect the droplet dynamics significantly, where τ is the relaxation time of fluid. Therefore, the coupling effect between the conformation of polymer chain and the shape of interface could be very important [5].

When the dispersed droplet becomes an anisotropic fluid, for example, a nematic liquid crystal, parameters such as the orientation of director, tumbling parameter of director, and the interfacial anchoring energy are going to affect the dynamics of the shape evolution of the droplet. The evolution of director not only changes the rheological properties of liquid crystal, it has direct influence on the shape of interface due to the presence of interfacial anchoring energy. However, less extensive works have been done to understand the effect of the director orientation and anchoring on the morphology evolution in flow field in a polymer-liquid-crystal system. Morphology evolution and rheological properties of systems containing LCs have been found to be different from flexible polymer systems in literature. Lishchuk *et al.* [6] investigated theoretically the shape of an isotropic droplet immersed in a nematic LC in the presence of an interfacial layer of surfactant and found, in a certain range of droplet sizes, the droplets are lens shaped and the aspect ratio dependent upon the ratio of anchoring strength and surface tension coefficients. Boussoualem *et al.* [7] studied the thermophysical, dielectric, and electro-optic properties of polymer-dispersed liquid crystal (PDLC) films. They observed an absorption domain in the dielectric spectrum of PDLC films at low frequency, and a drastic decrease in the optical transmittance of the film occurs. This phenomenon can be related to

*Corresponding author. Email address: wyu@sjtu.edu.cn

an interfacial polarization process resulting from a charge accumulation at the droplet-polymer interface. Lee *et al.* [8] studied the deformation and retraction of thermotropic liquid crystalline polymer droplets Vectra-B950 in a flexible polymer matrix, and the results showed that the initial deformation of the small liquid crystalline polymer droplets is smaller than that of the flexible polymer droplets. They attributed this phenomena to the effect of orientational elasticity in the liquid crystalline polymer. Riise *et al.* [9] investigated the rheological properties of blends of dispersed aqueous lyotropic liquid crystalline phase in isotropic polymer matrix, and they found the blends of 10% LCs could not follow the Palierne model but the blends of 20% LCs could. They explained that the difference came from the droplet sizes in two concentrations with respect to the scales of domain in LCs. The effect of interfacial anchoring of the nematic director on the linear viscoelasticity of LC/polymer blends has been revealed more clearly in our previous work by experiments and a simple model [10]. Gao *et al.* [11] reported experimental optical observations on the deformation, breakup, and coalescence of thermotropic liquid crystalline polymers (TLCP) embedded in a polypropylene matrix, and they revealed that the fiber formation and droplet deformation of TLCP are very dependent on the droplet size and viscosity ratio. These works are constructive and inspiring. However, the mechanism of morphology evolution of LC dispersion in a matrix is far from clear due to the complexity of LC structure.

In this paper we will investigate the behaviors of liquid crystal droplet deformation in two-dimensional (2D) linear transient flow and steady flow, and compare with the Newtonian ones, for a given viscosity ratio. We adopted the Yu Zhou (YZ) LC model to calculate the morphology evolution of LC droplets. This model is suitable to describe the coupling effects between the LC droplet shape, and the director, the LC droplet shape, and the conformation of polymer chain.

II. THEORETICAL MODEL

To describe the behavior of a Newtonian droplet in the other Newtonian matrix up to a limited deformation, the Maffettone-Minale (MM) model [12] can give a quite good prediction. For example, the deformation parameter D and orientation angle β for a single dispersed droplet can be written as

$$D = \frac{L-B}{L+B} = \frac{\sqrt{f_1^2 + \mathrm{Ca}^2(-1+\alpha)^2} - \sqrt{f_1^2 + \mathrm{Ca}^2(-1+\alpha)^2 - \mathrm{Ca}^2(1+\alpha)^2 f_2^2}}{\mathrm{Ca}(1+\alpha) f_2}, \tag{1}$$

$$\beta = \frac{1}{2}\tan^{-1}\frac{\mathrm{Ca}(-1+\alpha)}{f_1}, \tag{2}$$

where f_1 and f_2 are the functions of viscosity ratio and L and B are the length of two axes of droplet. α describes the type of flow field (see below). The MM model is incapable of describing a system where a fluid has certain microstructure, such as liquid crystal. To describe the behavior of a LC droplet, at least the microstructural evolution inside the LC droplet, its effect on the interfacial properties and the effect of interfacial properties on the shape of interface should be considered. Yu [13] proposed a model (the YZ-LC model) by the Hamiltonian approach, which has considered these effects in polymer-liquid crystal systems. On the assumption that the viscoelasticity of matrix can be neglected, the dynamic equation for the LC droplet shape can be written in a dimensionless form as

$$\begin{aligned}\frac{dG_{\alpha\beta}}{dt^*} &= \mathrm{Ca}(G_{\alpha\gamma}\omega_{\gamma\beta} - \omega_{\alpha\gamma}G_{\beta\gamma}) - f_{2s}\mathrm{Ca}(G_{\alpha\gamma}D_{\gamma\beta} + D_{\alpha\gamma}G_{\beta\gamma}) - g_{1s}\left(\frac{3G_{\alpha\gamma}G_{\beta\gamma}}{I_1(G)} - G_{\alpha\beta}\right) - \frac{\theta}{6}g_{2s}\Bigg[(1-m{:}G)I_2(G)2\Bigg(G_{\alpha\gamma}m_{\gamma\varepsilon}G_{\beta\varepsilon} \\ &\quad - \frac{1}{3}m{:}GG_{\alpha\beta}\Bigg) + [2m{:}G - (m{:}G)^2]\left(I_1(G)G_{\alpha\gamma}G_{\beta\gamma} - G_{\alpha\gamma}G_{\gamma\varepsilon}G_{\beta\varepsilon} - I_2(G)\frac{2}{3}G_{\alpha\beta}\right)\Bigg] + \frac{aq^2\varepsilon p_2}{2\lambda}\left(m_{\alpha\gamma}G_{\beta\gamma} + G_{\alpha\gamma}m_{\beta\gamma} - \frac{2}{3}G_{\alpha\beta}\right) \\ &\quad - 2aq\frac{\theta}{6}(1-m{:}G)I_2(G)[m_{\alpha\gamma}G_{\gamma\varepsilon}G_{\beta\varepsilon} + G_{\alpha\varepsilon}G_{\gamma\varepsilon}m_{\beta\gamma} - m{:}G(m_{\alpha\gamma}G_{\beta\gamma} + G_{\alpha\gamma}m_{\beta\gamma})],\end{aligned} \tag{3}$$

where G is the second-order tensor representing the ellipsoid morphology, Ca the capillary number, ω the asymmetric part of velocity gradient tensor, D the symmetric part of velocity gradient tensor, f the coupling parameter depending on the viscosity ratio, g the coefficients of functions of viscosity ratio and volume fraction, θ the ratio of anchoring energy due to the nematic orientation at interface to isotropic interfacial tension, m the second-order tensor to represent the conformation of long rodlike molecules of liquid crystal, a the coupling parameter of LC droplet, ε the dimensionless constant, q the ratio between the characteristic times of droplet shape and disclination texture, p the viscosity ratio between droplet viscosity and matrix viscosity, and λ the tumbling parameter of liquid crystal.

The coupling effect between nematic director and droplet shape can be described quite well by this model (see [13] for details). Among all the parameters in Eq. (3), the determinants include the viscosity ratio $p=\eta_d/\eta_m$ and $p_2=(\alpha_2+\alpha_3)/\eta_m$ (η_d and η_m are viscosity of droplet and matrix; α_2 and α_3 are two of the six Leslie viscosity coefficients), capillary number Ca, tumbling parameter λ, coupling parameter a, interface energy ratio θ, and $q=\rho_v\lambda_G$ (ρ_v is the volumetric disclination density inside the LC droplet and λ_G the characteristic relaxation time of LC droplet). In shear flows, the viscosities α_2 and α_3 determine director torques in the orientations. $\theta=\Gamma_{an}/\Gamma_0$ is the ratio of the anchoring energy to isotropic interfacial tension. θ is restricted to a value greater than −2 due to the positive requirement of interfacial free energy and isotropic interfacial tension. If $\theta=0$, the interfacial anisotropy vanishes; for $\theta>0$, the interface easy axis is parallel to the interface (planar anchoring); for $\theta<0$, the interface easy axis is perpendicular to the interface (homeotropic anchoring). Asymptotic analysis on weak shear flow [13] has shown that the tumble parameter λ of director and interface energy ratio θ have the most significant effects on the droplet deformation.

III. EXPERIMENTS

A. Materials

The low molar mass liquid crystal 4′-pentyl-4-biphenylcarbonitrile (5CB) and 4′-octyl-4-biphenylcarbonitrile (8CB) was purchased from Yantai valiant fine chemicals Co., Ltd. in China. 5CB undergoes a crystal-nematic transition at 22 °C and a nematic-isotropic transition at 36 °C. 8CB undergoes a crystal–smectic-*A* transition at 22 °C, a smectic-*A*–nematic transition at 34 °C, and a nematic-isotropic transition at 41 °C. The transitions can be readily determined by the differential scanning calorimeter or the polarized optical microscope. The matrix fluid PDMS was purchased from Shanghai resin plant of China and used without further purification. The molecular weight of PDMS is about 200 000. The zero-shear viscosity of PDMS was measured on a rotational rheometer (Bohlin Gemini 200HR) by using a 25 mm plate-plate geometry. The complex viscosities of 5CB at different temperatures are adopted data measured by Rai *et al.* [14]. The viscosity ratio p of our system is very small, about 4.5×10^{-4}. Although the viscosity of liquid crystal would probably change due to the evolution of texture during the droplet retraction, the corresponding change in viscosity of LC has little effect on the retraction process of a LC droplet. In fact, the retraction process of a Newtonian droplet immersed in another Newtonian matrix depends on a factor which is a function of the viscosity ratio, i.e., $f_1=40(p+1)/(2p+3)\times(19p+16)$, which only varies less than 1% when the viscosity ratio changes from 10^{-4} to 10^{-2}. So we think the effect of the change of viscosity ratio during the droplet retraction is very limited and can be neglected in our experiment.

B. Experimental apparatus

The experiments were performed in a computer controlled four roll mill. The rollers are independently driven by four stepping motors and vertically immersed in a cubic tank. The dimensions of a sample tank are about $60\times60\times75$ mm, and a single liquid crystal droplet range from about 0.10 to 0.50 mm in diameter was injected in the center of the matrix by using a syringe with a small needle. Channeling temperature-controlled water through the walls of the tank controls the temperature in the cell to within ±0.1 °C. The temperature is first raised high enough in the isotropic state, and then quenched to the test temperature in the liquid crystal state. Quenching from isotropic state to liquid-crystal state is believed to produce more consistent initial morphology of LC. The deformation and retraction of LC droplets are viewed using an optical microscope from the bottom of the four-roll mill and recorded through a CCD camera for real-time visualization. Quantitative information on the droplet shape is obtained by an automated procedure based on image analysis techniques. An image processing and analysis software is used to directly provide the continuous values of two axes of the ellipsoid droplet in the velocity-velocity gradient plane and the orientation angle of the droplet automatically.

IV. RESULTS AND DISCUSSIONS

The four-roll mill can produce an arbitrary linear flow field between simple shear and planar extensional flow, where the velocity can be described as

$$\mathbf{v}=(\nabla\cdot\mathbf{v})^T\cdot\mathbf{x}=\mathbf{L}\cdot\mathbf{x}, \tag{4}$$

where $\mathbf{x}$ is the position vector, $\mathbf{L}$ is the velocity-gradient tensor, and

$$\mathbf{L}=\frac{G}{2}\begin{bmatrix}1+\alpha & 1-\alpha & 0\\ -1+\alpha & -1-\alpha & 0\\ 0 & 0 & 0\end{bmatrix},\quad -1\leqslant\alpha\leqslant1, \tag{5}$$

where G is the scalar velocity gradient and α is the flow-type parameter. The flow-type parameter is a measure of the relative magnitude of strain rate to vorticity; e.g., $\alpha=1.0$ for purely extensional flow and $\alpha=0$ for simple shear flow. In this work the flow-type parameter is set as 1, 0.8, 0.6, 0.4, 0.2, and 0, respectively. The schematic diagram of the flow field produced by a four-roll mill is shown in Fig. 1, with the definition of the coordination system used in this work.

Both the MM model for Newtonian droplet and the YZ-LC model for nematic droplet are used to compare with the experiments. The parameters used in the YZ-LC model are obtained from our experiments and from literature [15,16]. The values of the viscosity of PDMS matrix, the radius of LC droplet, and the shear rate of steady flow in calculations are available from the experiments and set as 180 Pa s, about 100–300 μm, and 0.002–0.02 s^{-1}, respectively. A dimensionless parameter ε is the same as the definition by Larson [16] and fixed at the value 0.03. For the Leslie viscosities we use a set of values that are available from the literature of Jamieson [17]. The tumbling parameter is calculated by two of the six Leslie viscosity coefficients α_2 and α_3 as 1.1 for 5CB and 0.3 for 8CB. The ratio of the anchoring energy to isotropic interfacial tension θ set as −0.1

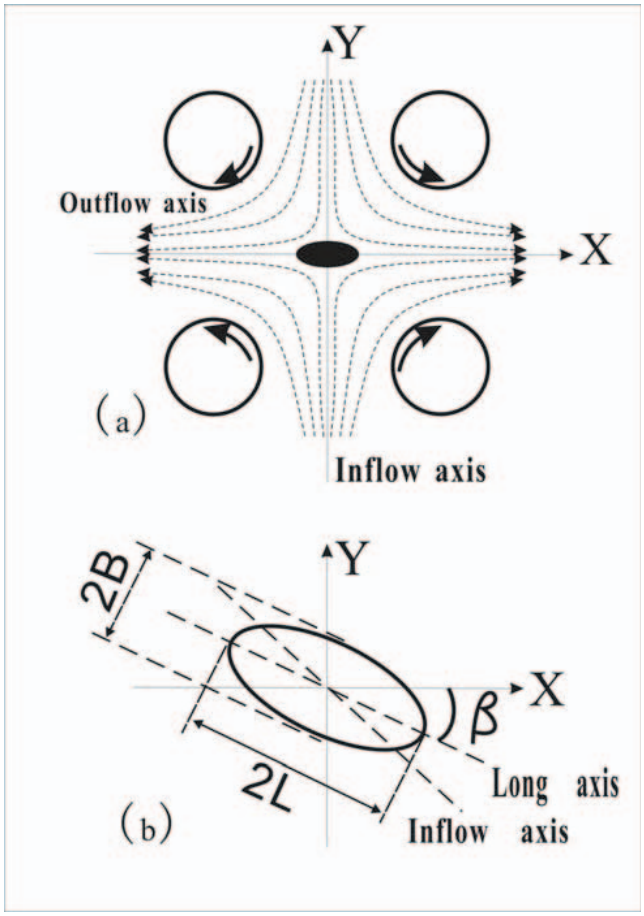

FIG. 1. (Color online) (a) Schematic diagram of the flow field produced by a four-roll mill with the definition of the coordination system used in the work; (b) orientation angle of the LC droplet with respect to the coordination system.

came from the data in literature [14,24] and the homeotropic surface anchoring [18,19]. Besides that, a coupling dimensionless constant, a, is unknown and set as 1 throughout this work.

A. Steady LC droplet deformation

In Fig. 2(a) the deformation parameter D, $D=(L-B)/(L+B)$, is plotted as a function of capillary number Ca (Ca $=\eta_m R\dot{\gamma}/\Gamma$) for steady data of 5CB (25 °C, nematic phase) and 8CB (36 °C, nematic phase) in extensional flow ($\alpha=1.0$). The interfacial tension Γ between LC and polymer matrix can be obtained by using the deformed droplet retraction method [20] from steady flow data of L and B of the droplet during retraction. In this work, the orientation angle β of the droplet refers to the angle of the long axis of ellipsoid droplet and horizontal axis, as shown in Fig. 1(b). The influence of droplet radius was considered and the data of different droplet sizes are totally coincident. The calculations of deformation parameter and orientation angle by the YZ-LC model and by the MM model are drawn by lines in Fig. 2. The deformation parameter in extensional flow in accordance with the calculation of the MM model when Ca

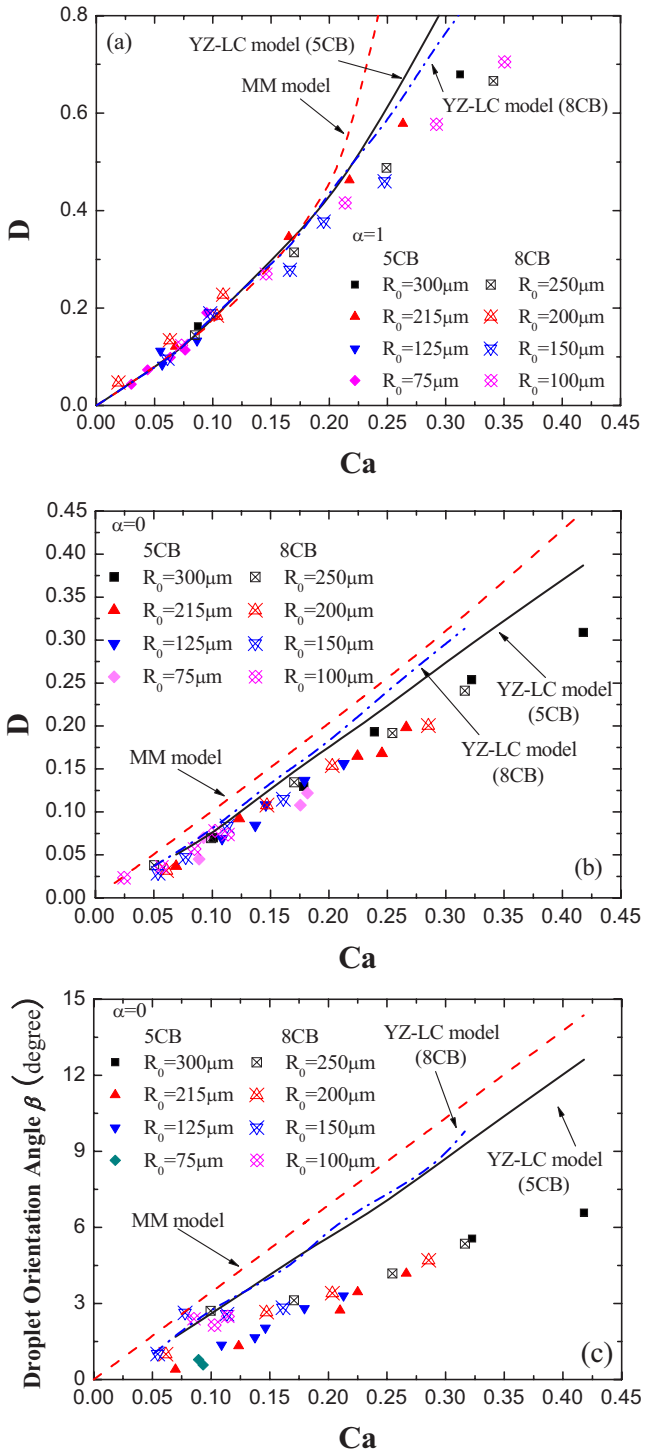

FIG. 2. (Color online) Steady LC droplet deformation parameter D and orientation angle β of 5CB and 8CB as a function of Ca (28 °C for 5CB and 36 °C for 8CB). (a) $\alpha=1$; (b), (c) $\alpha=0$.

is less than ~0.15 indicates that the deformation of the liquid-crystal droplet at low Ca is similar to that of the Newtonian droplets, i.e., the anisotropic and nematic properties of LC do not influence the LC deformation. It also seems that the flow-aligning 5CB and flow-tumbling 8CB do not exhibit a difference in deformation in Fig. 2.

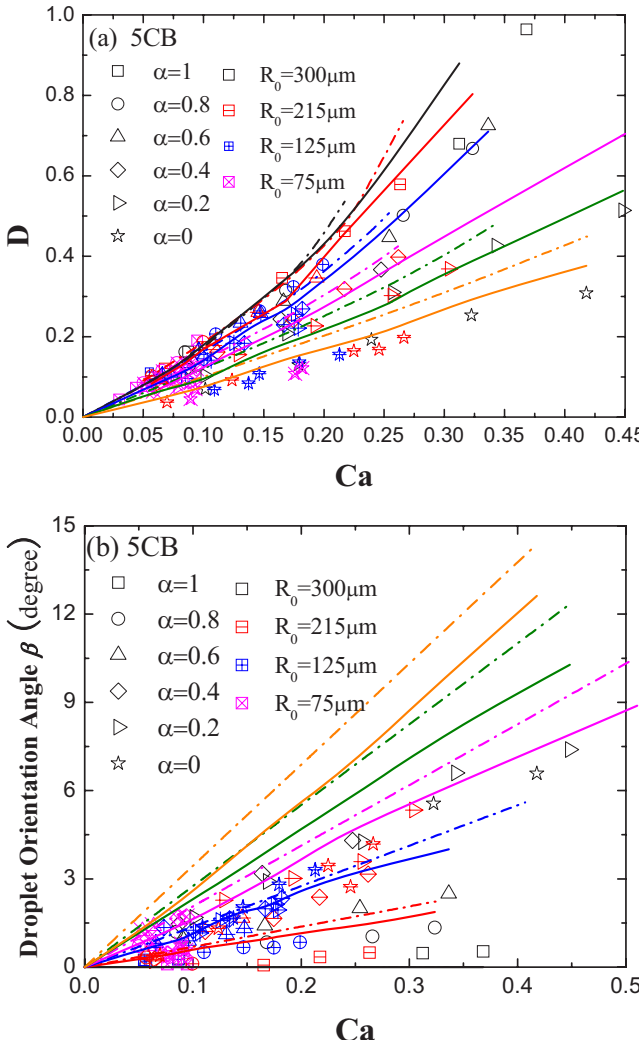

FIG. 3. (Color online) Comparison of experimental deformation parameter D and orientation angle β of 5CB for different radius with calculation by the MM model (dash-dot lines) and the YZ-LC model (solid lines) at steady state as a function of Ca (28 °C).

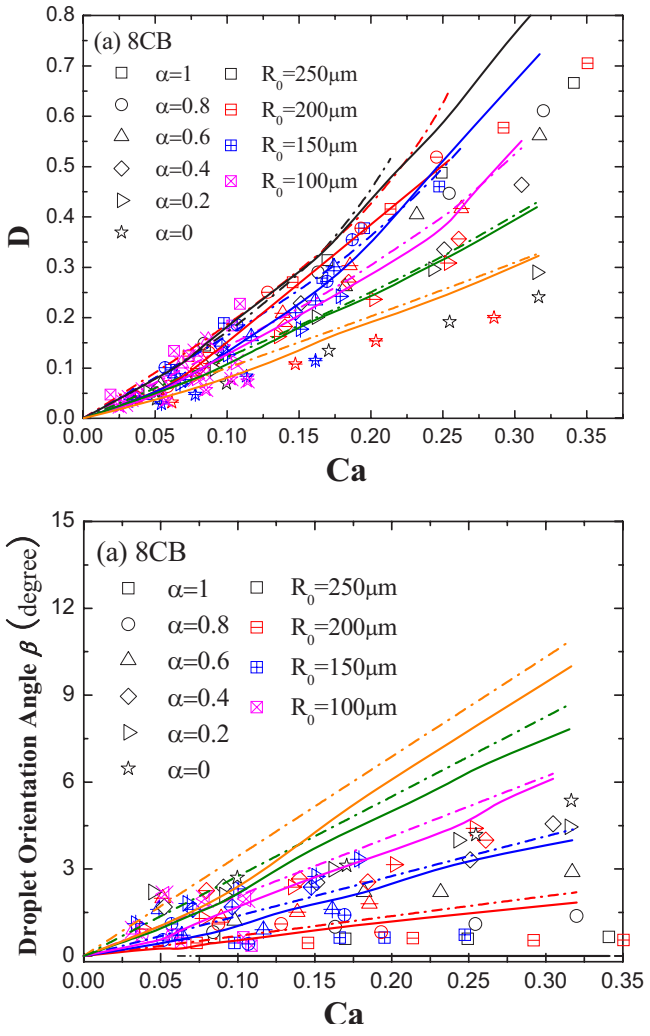

FIG. 4. (Color online) Comparison of experimental deformation parameter D and orientation angle β of 8CB for different radius with calculation by the MM model (dash-dot lines) and the YZ-LC model (solid lines) at steady state as a function of Ca (36 °C).

The effect of steady shear flow (α=0) on deformation and rotation of 5CB and 8CB droplets is shown in Figs. 2(b) and 2(c), respectively. We can see that the deformation of the LC droplet in simple shear flow is evidently smaller than calculation by the MM model, which fits the Newtonian droplets very well. This is probably induced by the LC's director changes in the simple shear flow. The orientation angle of the LC droplet in Fig. 2(c) also shows more difficult rotation of a LC droplet than a Newtonian droplet. The calculations in Fig. 2 by the YZ-LC model are better than calculations by the MM model both for droplet deformation and orientation angle. The trends of the predictions of the deformation parameter are basically identical to the experimental data; however, the predictions of orientation angle slightly deviate from the real values. Although it is expected that nematic behavior should have certain effects on LC droplet deformation, such an effect is not observed for the LC droplet size above tens of microns which is much larger than the scales of LC domains about several microns. Moreover, 5CB droplet and 8CB droplet do not show evident difference in steady droplet deformation and orientation, although the predictions by the YZ-LC model show a slight difference.

The steady deformation of the LC droplet in different flow type, a=0, 0.2, 0.4, 0.6, 0.8, and 1, was investigated and the deformation parameter of different 5CB radius were plotted in Fig. 3(a) and the orientation angle in Fig. 3(b) as a function of Ca. The dash-dotted lines and solid lines in Fig. 3 are the calculations by the MM model and by the YZ-LC model, respectively. Although the MM model can well describe the deformation of the Newtonian droplet, the discrepancy occurs while the dispersed droplet is liquid crystals. The calculations of the deformation parameter by using the MM model are a little less than the experimental data of Bentley *et al.* [21] for different viscosity ratio, whereas the calculations for LC/PDMS system by this model are obviously higher than the real values in our experiments, especially for the occasions of α=0. In Fig. 3(b), the calculated orientation angle by the MM model for LC/PDMS is much higher than the real one. From the comparison we can conclude that the deformation and rotation of the LC droplet is more difficult than

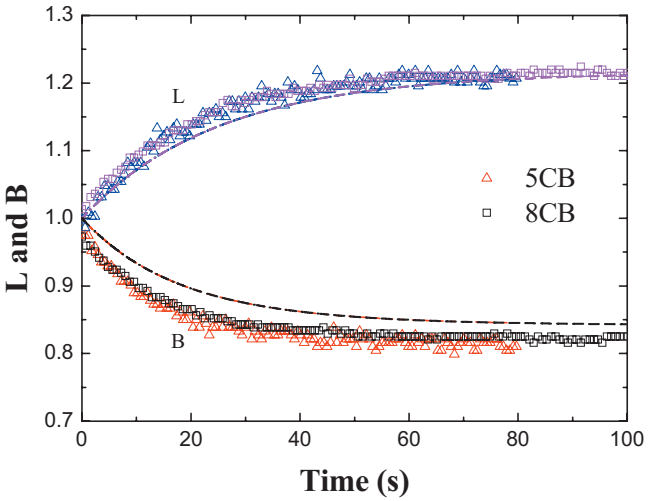

FIG. 5. (Color online) Comparison of two axes of transient deformation of 5CB and 8CB droplet in steady flow. (R_0=0.50 mm; G=0.006 s^{-1}; α=1), 28 °C for 5CB, and 36 °C for 8CB. The lines are predictions by the YZ-LC model.

Newtonian droplets, possibly because of the resistance of the nematic elastic energy induced from the nematic mesogens deformation and orientation under flow field. This is in accordance with the results of Lee *et al.* [8], who found the initial deformation of the small liquid crystalline polymer droplets deform less than that of the PET droplet. The solid lines in Fig. 3 are the calculations by the YZ-LC model for deformation parameter and orientation angle. Since the YZ-LC model integrates the effects of the LC droplet shape and the director, it can be seen that this model is better for describing the LC droplet deformation than the MM model both for 5CB deformation and orientation. The different radius of 8CB droplets in different flow type are shown in Fig. 4 with the calculations of the YZ-LC and MM models, and the situations are very similar to those of 5CB.

B. Transient behavior

Transient deformations of 5CB and 8CB droplet are shown in Fig. 5. The radius of 5CB and 8CB droplet and the strength of flow field were chosen almost the same. The calculated evolution of two axes of 5CB and 8CB are plotted in dashed lines in Fig. 5. It can be seen that the calculations of the long axis during deformation are basically close to the experimental results; nevertheless, the calculations of short axis in deformation are a little deviated from the real values.

The transient course of LC droplet deformation to a steady value are recorded and the different radius dependence shown in Figs. 6(a) and 6(b) are the different droplets deformation in steady flow for 5CB and 8CB, respectively. The calculations by the YZ-LC model are drawn by lines. In order to compare the process of deformation, the data of same steady value are chosen. The different droplet 5CB show different deformation curves, as shown in Fig. 7(a); the smaller the LC droplet, the faster it reaches a steady deformation. The experiments of 8CB in Fig. 7(b) are less apparent than 5CB, but the same trend can still be found from

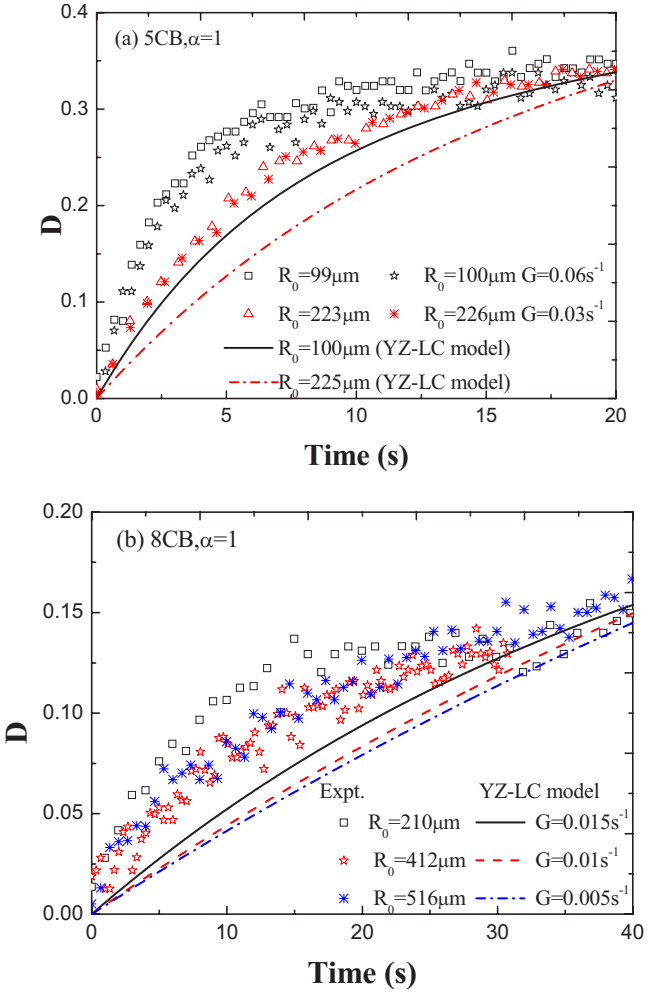

FIG. 6. (Color online) Dependence of LC droplet sizes on the deformation process in steady flow for (a) 5CB and (b) 8CB, 28 °C for 5CB and 36 °C for 8CB, with comparison of calculations by the YZ-LC model.

more scattered data. Even though the calculations by the YZ-LC model deform slower than the experimental LC droplets, the calculations for 5CB and 8CB show the dependence of droplet size on deformation rate.

It is known that 5CB and 8CB behave differently under shear flow. The director of 5CB shows flow-aligning behavior, while the director of 8CB shows tumbling behavior. The nematic tumbling instability of 8CB attributed to the director is forced to rotate continuously by hydrodynamic torques when subjected to a shear flow, whereas the director of 5CB shows flow-aligning behavior, i.e., the director aligns at a characteristic angle with respect to the flow direction [22,23]. However, the effect of director tumbling of 8CB seems unable to be observed in our experiments. We try to see whether different behavior of the director can be predicted by the YZ-LC model, and the results are as shown in Fig. 7. The calculated director inside the 5CB droplet shows flow-aligning behavior that gradually reaches a steady value for a given Ca with different radius of the LC droplet R_0 =1 μm, 10 μm, and 100 μm. The calculated director of 8CB shows apparent tumbling behavior when the radius of

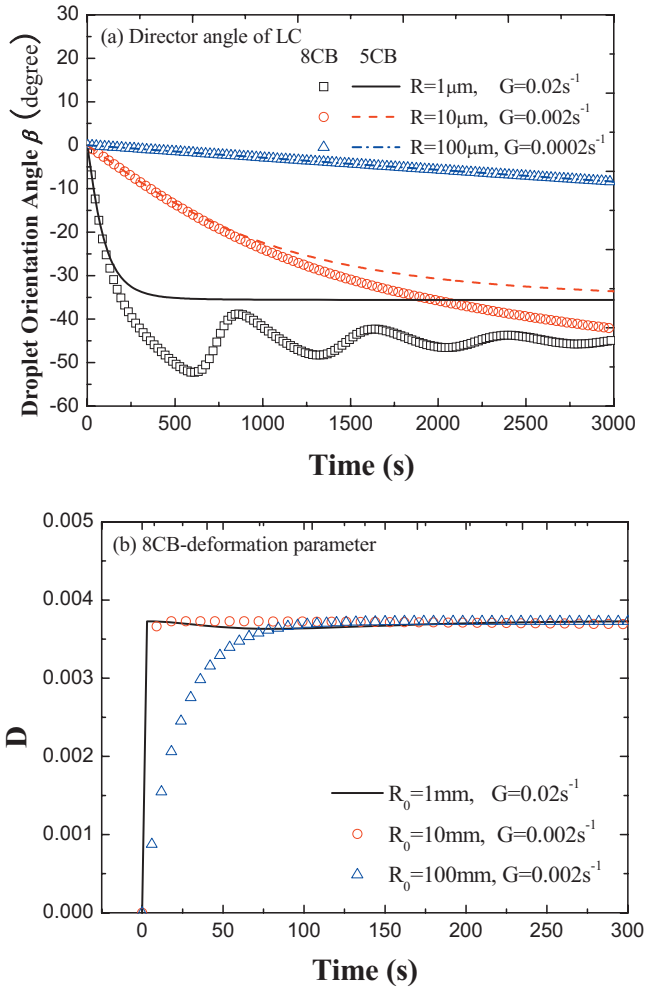

FIG. 7. (Color online) Calculation of the director angle of (a) 5CB and 8CB by the YZ-LC model at a constant Ca. (b) Calculation of the deformation parameter of 8CB droplet.

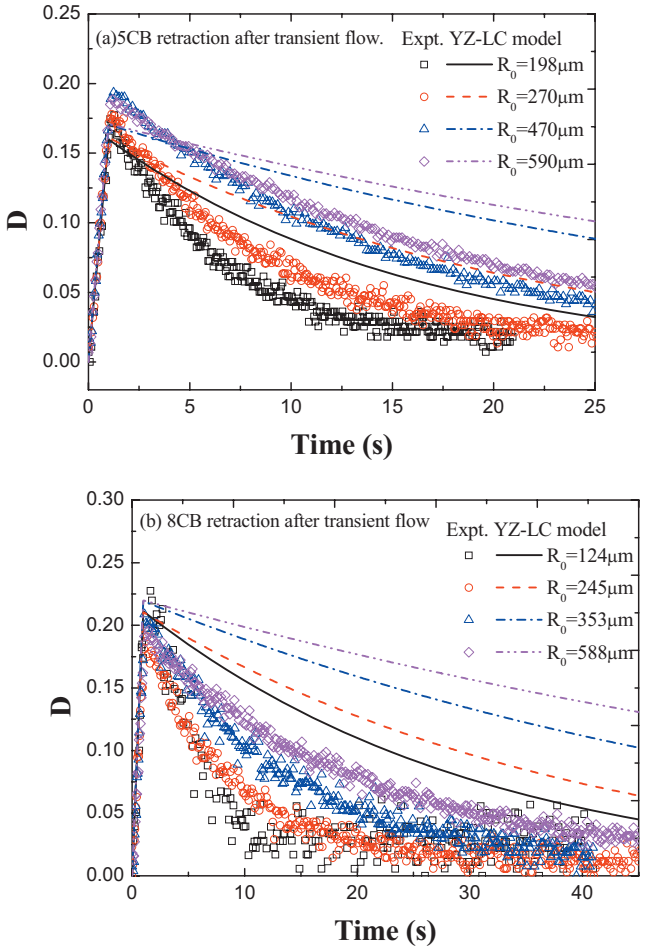

FIG. 8. (Color online) Retraction processes of ellipsoid LC droplet are plotted in Fig. 9 for (a) 5CB and (b) 8CB as a function of time in transient flow. (α=1, 28 °C for 5CB, and 36 °C for 8CB.)

LC is 1 μm, which is very close to the scale of domain size of several microns, while the tumbling disappears when the radius of 8CB increases more than 10 μm. Figure 7(b) is the corresponding deformation parameter of the 8CB droplet by the YZ-LC model. It can be seen that even on the occasion of R_0=1 μm, the calculated D does not exhibit obvious change during deformation, which means that the tumbling behavior of the director has quite a small effect on the transient droplet deformation. In our experiments, the minimum droplet radius is much larger than 10 μm, therefore the tumbling behavior cannot be reflected by our experiments for 8CB.

C. LC droplet retraction

Besides the steady flow, we also investigate the LC droplet deformation and retraction in transient flow (the flow field is applied only 1 s). The retraction processes of ellipsoid LC droplet are plotted in Fig. 8 for (a) 5CB and (b) 8CB as a function of time in transient flow. Different droplet sizes of LC are compared and the calculations by the YZ-LC model are shown in Fig. 8. The initial deformation parameters of different LC droplets are controlled to be almost the same. The retraction processes are greatly dependent on the droplet radius. The smaller droplets retract faster than the bigger ones. The calculations by the YZ-LC model exhibits the radius dependence, however, the calculations do not fit the experiments very well, especially for 8CB droplets retraction.

The retraction process of LC droplet in transient flow and steady flow is reflected by deformation parameter D versus time in Fig. 9(a), for 5CB and Fig. 9(b) for 8CB. The initial deformation parameter of transient flow and steady flow is controlled to be the same value equal to 0.10 and 0.20. The transient flow curve is shifted along x coordinate in order to compare the retraction process with the steady data. It appears from Fig. 10 that the retraction curves can be basically superimposed for steady and transient data, which means the dynamic evolution of the LC droplet in retraction is the same for transient and steady flow. The superpositioned curves seem not to be consistent with the idea that the retraction process would be different after applying transient flow and steady flow due to the reorientation of nematic structure on the surface and in the bulk of the droplet undergo different flow experience during deformation. This may be because the nematic orientation in the LC droplet will reach a bal-

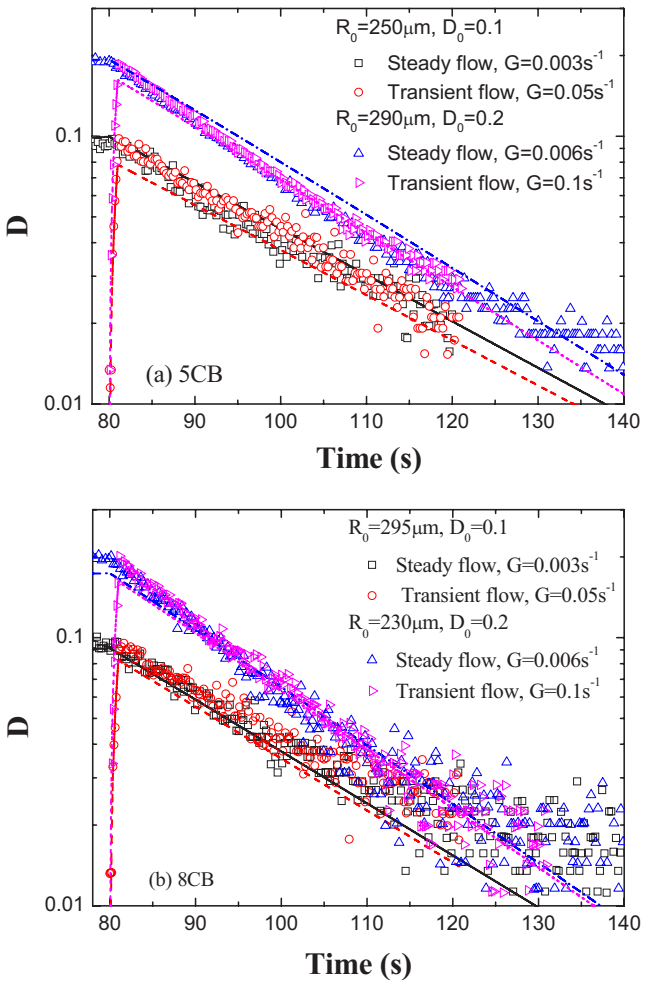

FIG. 9. (Color online) Deformation parameter (D_0=0.10; D_0 =0.20) of 5CB and 8CB during droplet retraction in transient flow and steady flow (flow type parameter α=1, 28 °C for 5CB, and 36 °C for 8CB). The lines are predictions of the YZ-LC model.

anced value under a certain strong flow field, both for a strong flow that lasts 1 s in transient flow and a weak flow that lasts 100 s in steady flow, and the balanced nematic orientation induces nearly the same retraction curves. The lines in Fig. 10 are the calculations of droplet retraction by the YZ-LC model for steady flow and transient flow, and the curves are basically in accord with the experimental data. Figure 10 is the comparison of the retraction process of 5CB and 8CB droplets at D_0=0.1. The calculations by the YZ-LC model show some difference between 5CB and 8CB droplets during retraction; however, such minor differences cannot be reflected by our experiment due to the scattered data points in the late stage of retraction.

V. CONCLUSIONS

In this work, we investigated deformation and retraction of a single low molar mass liquid-crystal 5CB and 8CB droplet dispersed in a PDMS matrix under 2D linear flow by

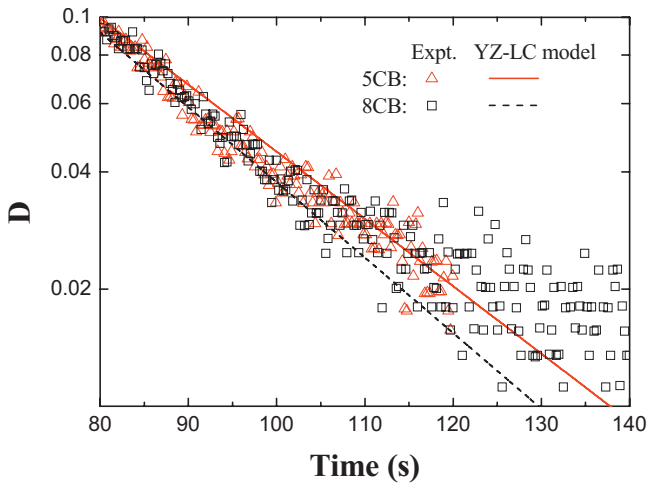

FIG. 10. (Color online) Comparison of the deformation parameter (D_0=0.10) between 5CB and 8CB during droplet retraction after transient flow and steady flow (flow type parameter α=1, R_0 ≈300 μm, 28 °C for 5CB, and 36 °C for 8CB). The lines are predictions of the YZ-LC model.

a computer-controlled four-roll mill, which is equipped with an optical microscope and a digital camera. The deformation parameter and orientation angle during deformation versus capillary number was obtained and compared with calculations using the MM and YZ-LC models. The results showed that the deformation and rotation of the LC droplet is more difficult than Newtonian droplets, possibly because of the resistance of the nematic elastic energy induced by the nematic mesogens deformation and orientation under flow field. The calculations of the YZ-LC model are found to be better for describing the LC droplet deformation than the calculations of the MM model since the former integrate the coupling effects between the LC droplet shape and the director and the LC droplet shape and the conformation of the polymer chain. In addition, the deformation and retraction of flow-aligning 5CB and flow-tumbling 8CB droplets were discussed by experiment and calculation. The different behavior between 5CB and 8CB could not be observed in our experiments; however, the YZ-LC model can predict the oscillating behavior of an 8CB director when the radius of LC is close to the scale of domain size of several microns. Moreover, the influence of droplet size of LC on deformation and retraction were discussed and the results reveal that the different droplet LC show different evolution curves: The smaller the LC droplet, the faster it reaches a steady state in deformation and retracts to a sphere drop. The calculations by the YZ-LC model for 5CB and 8CB show the obvious dependence of droplet size on deformation rate.

ACKNOWLEDGMENTS

This work was supported by research grants from the National Natural Science Foundation of China (No. 20674051, No. 20490220, and No. 20474039).

[1] P. K. Ray, Ph.D. thesis, City University of New York, 2004.
[2] J. M. Rallison, Annu. Rev. Fluid Mech. **16**, 45 (1984).
[3] H. A. Stone, Annu. Rev. Fluid Mech. **26**, 65 (1994).
[4] S. Guido and M. Villone, J. Rheol. **42**, 395 (1998).
[5] W. Yu and C. X. Zhou, J. Rheol. **49**, 215 (2005).
[6] S. V. Lishchuk and C. M. Care, Phys. Rev. E **70**, 011702 (2004).
[7] M. Boussoualem and F. Roussel, Phys. Rev. E **69**, 031702 (2004).
[8] H. S. Lee and M. M. Denn, J. Non-Newtonian Fluid Mech. **93**, 315 (2000).
[9] B. L. Riise, N. Mikler, and M. M. Denn, J. Non-Newtonian Fluid Mech. **86**, 3 (1999).
[10] W. Yu, Y. J. Wu, R. B. Yu, and C. X. Zhou, Rheol. Acta **45**, 105 (2005).
[11] P. Gao, M. R. Mackley, and D. F. Zhao, J. Non-Newtonian Fluid Mech. **80**, 199 (1999).
[12] P. L. Maffettone and M. Minale, J. Non-Newtonian Fluid Mech. **78**, 567 (1998).
[13] W. Yu and C. X. Zhou, J. Chem. Phys. **123**, 014906 (2005).
[14] P. K. Rai, M. M. Denn, and C. Maldarelli, Langmuir **19**, 7370 (2003).
[15] A. D. Gotsis and M. A. Odriozola, J. Rheol. **44**, 1205 (2000).
[16] R. G. Larson and M. Doi, J. Rheol. **35**, 539 (1991).
[17] A. M. Jamieson, D. Gu, F. L. Chen, and S. Smith, Prog. Polym. Sci. **21**, 981 (1996).
[18] Y. J. Wu, W. Yu, and C. X. Zhou, J. Colloid Interface Sci. **303**, 546 (2006).
[19] Jian Wu and P. T. Mather, Macromolecules **38**, 7343 (2005).
[20] H. Y. Mo, C. X. Zhou, and W. Yu, J. Non-Newtonian Fluid Mech. **91**, 221 (2000).
[21] B. J. Bentley and L. G. Leal, J. Fluid Mech. **167**, 241 (1986).
[22] N. Yao and A. M. Jamieson, Macromolecules **31**, 5399 (1998).
[23] I. Quijada-Garrido, H. Siebert, C. Friedrich, and C. Schmidt, Macromolecules **33**, 3844 (2000).
[24] S. Faetti and P. Marianelli, Phys. Rev. E **72**, 051708 (2005).